

Studies on magneto-electro-elastic cantilever beam under thermal environment

P. Kondaiah, K. Shankar* and N. Ganesan

Machine Design Section, Department of Mechanical Engineering, Indian Institute of Technology,
Madras, Chennai 600 036, India

(Received April 30, 2012, Revised June 12, 2012, Accepted June 13, 2012)

Abstract. A smart beam made of magneto-electro-elastic (MEE) material having piezoelectric phase and piezomagnetic phase, shows the coupling between magnetic, electric, thermal and mechanical under thermal environment. Product properties such as pyroelectric and pyromagnetic are generated in this MEE material under thermal environment. Recently studies have been published on the product properties (pyroelectric and pyromagnetic) for magneto-electro-thermo-elastic smart composite. Hence, the magneto-electro-elastic beam with different volume fractions, investigated under uniform temperature rise is the main aim of this paper, to study the influence of product properties on clamped-free boundary condition, using finite element procedures. The finite element beam is modeled using eight node 3D brick element with five nodal degrees of freedom *viz.* displacements in the x , y and z directions and electric and magnetic potentials. It is found that a significant increase in electric potential observed at volume fraction of $BaTiO_3$, $v_f=0.2$ due to pyroelectric effect. In-contrast, the displacements and stresses are not much affected.

Keywords: magneto-electro-elastic; pyroelectric; pyromagnetic; finite element; thermal environment

1. Introduction

A smart composite magneto-electro-elastic (MEE) material having piezoelectric phase and piezomagnetic phase exhibits the coupling between mechanical, electrical and magnetic fields. This unique class of smart composite consisting of a piezoelectric phase shows a coupling between mechanical and electric fields whereas the piezomagnetic phase shows the coupling between mechanical and magnetic fields. Along with this, a magneto-electric coupling effect, which is absent in the constituent phases, is exhibited by these classes of magneto-electro-elastic materials. Under thermal environment MEE composites also exhibits product properties (pyroelectric and pyromagnetic), which are not present without a thermal field. Due to the exceptional nature of these materials, if developed, could find widespread applications in medical ultrasonic imaging, magnetic field probes, acoustic devices, sensors and actuators.

Gu *et al.* (2000) has developed a higher order temperature theory for coupled thermo-piezoelectric-mechanical modeling of smart composite consisting PZT and graphite. Pan (2001) studied the exact

* Corresponding author, Dr., E-mail: skris@iitm.ac.in

solutions for three dimensional, anisotropic, linearly magneto-electro-elastic, simply supported and multilayered plates under internal and surface loads. The solutions were expressed in terms of propagator matrix and concluded that the response from an internal load was quite different from surface load for relatively thin plate. Gornandt and Gabbert (2002) have presented finite element analysis of thermopiezoelectric smart structures with fully coupled formulation for static and dynamic response under combined thermal, electric and mechanical excitations. Aboudi (2001) has presented the effective moduli of magneto-electro-elastic composite by employing homogenization method with the assumption that composites have a periodic structure. Sunar *et al.* (2002) has presented finite element modeling of a fully coupled thermopiezomagnetic continuum with the aid of thermodynamic potential. A general coupled field finite element formulation for thermopiezomagnetic smart structures was derived by using the variational approach. Buchanan (2004) used a three dimensional vibrating infinite plate problem to study the influence of magneto-electro-elastic constants obtained by combining $BaTiO_3$ and $CoFe_2O_4$. Ootao and Tanigawa (2005) have analyzed the multilayered magneto-electro-thermoelastic composite strip under nonuniform heat across width direction and presented transient behavior of two-dimensional temperature by using Laplace and finite sine transformations. Kumaravel *et al.* (2007) has presented the steady state analysis of a MEE strip under thermal environment on two dimensional rectangular element without considering pyroelectric and pyromagnetic coupling effects. Pan *et al.* (2009) has presented the effects of geometric size and mechanical boundary conditions on magneto-electric coupling in by-layered composites using 3D finite element approach. Alibeigloo (2010) studied thermoelasticity analysis of functionally graded beam with integrated surface piezoelectric layers under an applied electric field and thermo-mechanical load. Huang *et al.* (2010) has presented the analytical and semi-analytical solutions of functionally graded magneto-electro-elastic beams subjected to arbitrary load, which was expanded in terms of sinusoidal series. Biju *et al.* (2011) has presented response analysis of multiphase magneto-electro-elastic sensors using 3D magnetic vector potential approach for different volume fraction of $BaTiO_3$.

Ootao and Ishihara (2011) have presented the exact solution of transient thermal stress problem of the multilayered magneto-electro-thermoelastic hollow cylinder in plane strain state under unsteady and uniform surface heating. Additionally they have investigated the stacking sequence, position of the interface on the stresses, electric potential and magnetic potential, and the effects of coupling between magnetic, electric and thermoelastic fields only without considering the influence of product properties. To the best of the author's knowledge, the influence of pyroelectric and pyromagnetic properties on magneto-electro-elastic beam under uniform temperature has not yet been reported. Hence this work attempts to study pyroelectric and pyromagnetic effects on MEE structure to account the thermal environment for enhancing the performance of MEE devices.

Recently Challagulla and Georgiades (2011) have presented product properties such as pyroelectric and pyromagnetic in micromechanical analysis of magneto-electro-thermo-elastic smart composite by using asymptotic homogenization method (which is an approximate method). There are disagreements in the results of Bravo-Castillero *et al.* (2008), and Challagulla and Georgiades (2011) even though both have used the same method. Whereas Kim (2011) presented the same effective properties by using an exact matrix method. There is partial agreement with those of Challagulla and Georgiades (2011). Hence in the present work Kim (2011) results are considered to study the influence of product properties pyroelectric and pyromagnetic on displacements, electric potential, magnetic potential, stresses, electric displacements and magnetic flux densities of a 3D magneto-electro-elastic beam.

2. Theoretical formulation

2.1 Constitutive equations

The thermodynamic potential for magneto-electro-thermo-elastic beam in a rectangular Cartesian coordinate system (x,y,z) as shown in Fig. 1, can be written from Sunar *et al.* (2002) as

$$G(S, E, H, \theta) = \frac{1}{2}S^T cS - \frac{1}{2}E^T \varepsilon E - \frac{1}{2}H^T \mu H - S^T eE - S^T qH - H^T mE - E^T p\theta - S^T \beta\theta - H^T \tau\theta \quad (1)$$

where S , E , H , and θ are strain, electric field, magnetic field and uniform temperature rise respectively. The quantities c , ε , μ , e , q , m , are elastic, dielectric, magnetic permeability, piezoelectric, piezomagnetic, and magnetoelectric coefficients respectively. β , p and τ are thermal expansion, pyroelectric and pyromagnetic constants respectively. Consequently, the constitutive relations are

$$\left. \begin{aligned} \sigma &= \frac{\partial G}{\partial S} = cS - eE - qH - \beta\theta \\ D &= -\frac{\partial G}{\partial E} = e^T S + \varepsilon E + mH + p\theta \\ B &= -\frac{\partial G}{\partial H} = q^T S + mE + \mu H + \tau\theta \end{aligned} \right\} \quad (2)$$

These equations relate stress σ , electric displacement D , and magnetic flux density B , to strain S , electric field E , and magnetic field H . Linear coupling is assumed between magnetic, electric, thermal and elastic fields.

2.2 Finite element modeling

A finite element formulation of a coupled system would be similar to that given in Biju *et al.* (2011). It is written; for displacements $\{u\} = \{u_x, u_y, u_z\}^T$, electrical potential $\{\Phi\}$ and magnetic potential $\{\psi\}$ within element in terms of suitable shape functions

$$\left. \begin{aligned} u &= [N_u] \{u^e\} \\ \phi &= [N_\phi] \{\phi^e\} \\ \psi &= [N_\psi] \{\psi^e\} \end{aligned} \right\} \quad (3)$$

Here N_u , N_ϕ and N_ψ are shape functions for mechanical, electric and magnetic field respectively and u^e , ϕ^e , and ψ^e are the elemental nodal displacement, electric potential and magnetic potential

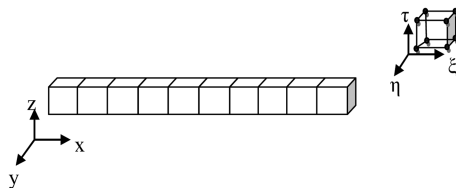


Fig. 1 Finite element discretization of magneto-electro-elastic beam

vectors. These shape functions for eight noded isoparametric element in natural coordinate (ξ, η, τ) system are given as follows

$$N_i(\xi, \eta, \tau) = \frac{1}{8}(1 + \xi\xi_i)(1 + \eta\eta_i)(1 + \tau\tau_i) \quad i = 1,2,\dots,8$$

where ξ , η and τ are the natural coordinates.

The strains can be related to the nodal degree of freedom by the following expression

$$\{S\} = [B_u]\{u^e\} \quad (4)$$

where $[B_u]$ is strain displacement matrix

The array of electric field vector is given by

$$\{E\} = \left\{ -\frac{d\phi}{dx} -\frac{d\phi}{dy} -\frac{d\phi}{dz} \right\} \quad (5)$$

The electric field vector can be related to electric potential as a nodal degree of freedom using the following expression as

$$\{E\} = [B_\phi]\{\phi^e\} \quad (6)$$

where $[B_\phi]$ is derivative of shape function matrix.

The array of magnetic field vector is given by

$$\{H\} = \left\{ -\frac{\partial\psi}{\partial x} -\frac{\partial\psi}{\partial y} -\frac{\partial\psi}{\partial z} \right\} \quad (7)$$

The magnetic field vector $\{H\}$ can be related to the magnetic potential as a nodal degree of freedom the following expression

$$\{H\} = [B_\psi]\{\psi^e\} \quad (8)$$

where $[B_\psi]$ is derivative of shape function matrix.

The different derivative of shape function matrices can be written with respect to eight node brick element as

$$[B_\phi] = [B_\psi] = \begin{bmatrix} \frac{dN_1}{dx} & \frac{dN_2}{dx} & \dots & -\frac{dN_8}{dx} \\ \frac{dN_1}{dy} & \frac{dN_2}{dy} & \dots & -\frac{dN_8}{dy} \\ \frac{dN_1}{dz} & \frac{dN_2}{dz} & \dots & -\frac{dN_8}{dz} \end{bmatrix} \quad [B_u] = \begin{bmatrix} \frac{dN_1}{dx} & 0 & 0 & \dots \\ 0 & \frac{dN_1}{dy} & 0 & \dots \\ 0 & 0 & \frac{dN_1}{dz} & \dots \\ \frac{dN_1}{dy} & \frac{dN_1}{dx} & 0 & \dots \\ 0 & \frac{dN_1}{dz} & \frac{dN_1}{dy} & \dots \\ \frac{dN_1}{dz} & 0 & \frac{dN_1}{dx} & \dots \end{bmatrix}$$

2.2.1 Evaluation of elemental matrices

The finite element equations for magneto-electro-elastic solid under thermal environment can be written as follows (Sunar *et al.* 2002)

$$\left. \begin{aligned} [K_{uu}^e]\{u^e\} + [K_{u\phi}^e]\{\phi^e\} + [K_{u\psi}^e]\{\psi^e\} - [K_{u\theta}^e]\{\theta^e\} &= \{F_u^e\} \\ [K_{\phi u}^e]\{u^e\} - [K_{\phi\phi}^e]\{\phi^e\} - [K_{\phi\psi}^e]\{\psi^e\} + [K_{\phi\theta}^e]\{\theta^e\} &= \{F_\phi^e\} \\ [K_{\psi u}^e]\{u^e\} - [K_{\psi\phi}^e]\{\phi^e\} - [K_{\psi\psi}^e]\{\psi^e\} + [K_{\psi\theta}^e]\{\theta^e\} &= \{F_\psi^e\} \end{aligned} \right\} \quad (9)$$

To investigate the pyroelectric and pyromagnetic effects, it is assumed that temperature of the system is uniform and does not fully couple with the magneto-electro-elastic field. Hence, Eq. (9) can be written as

$$\left. \begin{aligned} [K_{uu}^e]\{u^e\} + [K_{u\phi}^e]\{\phi^e\} + [K_{u\psi}^e]\{\psi^e\} &= \{F_u^e + F_{u\theta}^e\} \\ [K_{\phi u}^e]\{u^e\} - [K_{\phi\phi}^e]\{\phi^e\} - [K_{\phi\psi}^e]\{\psi^e\} &= \{F_\phi^e - F_{\phi\theta}^e\} \\ [K_{\psi u}^e]\{u^e\} - [K_{\psi\phi}^e]\{\phi^e\} - [K_{\psi\psi}^e]\{\psi^e\} &= \{F_\psi^e - F_{\psi\theta}^e\} \end{aligned} \right\} \quad (10)$$

where $\{F_u^e\}$, $\{F_\phi^e\}$ and $\{F_\psi^e\}$ corresponds to elemental applied mechanical force, electric charge and magnetic current vectors respectively.

In the present study, temperature is considered as the known quantity and hence the thermal load term, and pyroelectric (electric load generated due to temperature) and pyromagnetic (magnetic load generated due to temperature) load terms can be treated as external loadings in the system equations. These can be solved for displacements, electric potential and magnetic potential. These external vectors used in system equations are given as follows

$$\{F_{u\theta}^e\} = \int_v [B_u]^T [c] [\beta] \theta dv \quad (11)$$

where $\{F_{u\theta}^e\}$ is thermal force vector.

$$\{F_{\phi\theta}^e\} = \int_v [B_\phi]^T [p] \theta dv \quad (12)$$

where $\{F_{\phi\theta}^e\}$ is pyroelectric force vector and negative sign in Eq. (10) is taken care by pyroelectric property in Table 1.

$$\{F_{\psi\theta}^e\} = \int_v [B_\psi]^T [\tau] \theta dv \quad (13)$$

where $\{F_{\psi\theta}^e\}$ is pyromagnetic force vector and negative sign in Eq. (10) is taken care by pyromagnetic property in Table 1.

The coupled formation of Eq. (10) without considering the applied mechanical force, electric charge and magnetic current can be written as

$$\begin{bmatrix} K_{uu} & K_{u\phi} & K_{u\psi} \\ K_{\phi u} & -K_{\phi\phi} & -K_{\phi\psi} \\ K_{\psi u} & -K_{\psi\phi} & -K_{\psi\psi} \end{bmatrix} \begin{Bmatrix} u \\ \phi \\ \psi \end{Bmatrix} = \begin{Bmatrix} F_{u\theta} \\ F_{\phi\theta} \\ F_{\psi\theta} \end{Bmatrix} \quad (14)$$

Table 1 Material properties of multiphase magneto-electro-elastic ($BaTiO_3-CoFe_2O_4$) composite *w.r.t.* different volume fraction (v_f) of $BaTiO_3$, and PZT 5A [Aboudi 2001, Kim 2011, Biju *et al.* 2011]

	0.0 v_f	0.2 v_f	0.4 v_f	0.5 v_f	0.6 v_f	0.8 v_f	1.0 v_f	PZT-5A
Elastic constants								
$C_{11}=C_{22}$ (GPa)	286	250	225	220	200	175	166	99.2
C_{12} (GPa)	173	146	125	120	110	100	77	54.01
$C_{13}=C_{23}$ (GPa)	170	145	125	120	110	100	78	50.77
C_{33} (GPa)	269.5	240	220	215	190	170	162	86.85
$C_{44}=C_{55}$ (GPa)	45.3	45	45	45	45	50	43	21.1
C_{66} (GPa)	56.5	52	50	50	45	37.5	44.5	22.6
Piezoelectric constants								
$e_{31}=e_{32}$ (C/m ²)	0	-2.0	-3.0	-3.7	-3.5	-4.0	-4.4	-7.20
e_{33} (C/m ²)	0	4.0	7.0	9.0	11.0	14.0	18.6	15.11
$e_{24}=e_{15}$ (C/m ²)	0	0	0	0	0	0	11.6	12.32
Dielectric constants								
$\epsilon_{11}=\epsilon_{22}$ ($10^{-9}C^2/N m^2$)	0.08	0.33	0.8	0.85	0.9	1.0	11.2	1.53
ϵ_{33} ($10^{-9}C^2/N m^2$)	0.093	2.5	5.0	6.3	7.5	10.0	12.6	1.5
Magnetic permeability constants								
$\mu_{11}=\mu_{22}$ ($10^{-4}Ns^2/C^2$)	-5.9	-3.9	-2.5	-2.0	-1.5	-0.8	0.05	0
μ_{33} ($10^{-4}Ns^2/C^2$)	1.57	1.33	1.0	0.9	0.75	0.5	0.1	0
Piezomagnetic constant								
$q_{31}=q_{32}$ (N/A m)	580	410	300	350	200	100	0	0
q_{33} (N/A m)	700	550	380	320	260	120	0	0
$q_{24}=q_{15}$ (N/A m)	560	340	220	200	180	80	0	0
Magnetoelectric constants								
$m_{11}=m_{22}$ ($10^{-12} N s/V C$)	0	2.8	4.8	5.5	6.0	6.8	0	0
m_{33} ($10^{-12} N s/V C$)	0	2000	2750	2600	2500	1500	0	0
Pyroelectric constants								
p_2 ($10^{-7} C/m^2K$)	0	-3.5	-6.5	-7.8	-9	-10.8	0	
Pyromagnetic constants								
τ_2 ($10^{-5} C/m^2 K$)	0	-36	-28	-23	-18	-8.5	0	0
Thermal expansion coefficient								
$\beta_{11}=\beta_{22}$ ($10^{-6} 1/K$)	10	10.8	11.8	12.3	12.9	14.1	15.7	2.2
β_{33} ($10^{-6} 1/K$)	10	9.3	8.6	8.2	7.8	7.2	6.4	2.2
Density								
ρ (kg/m ³)	5300	5400	5500	5550	5600	5700	5800	7750

where the matrices $K_{u\phi}$ and $K_{\phi u}$ are stiffness matrices due to piezoelectric-mechanical coupling effect, and $K_{u\psi}$ and $K_{\psi u}$ are stiffness matrices due to piezomagnetic-mechanical coupling effect, and $K_{\phi\psi}$ and $K_{\psi\phi}$ are stiffness matrices due to electro-magnetic and magneto-electric coupling effects. $K_{u\theta}$, $K_{\phi\theta}$ and $K_{\psi\theta}$ are stiffness matrices due to thermal-mechanical, thermal-electrical and thermal-magnetic couplings, respectively. The matrices K_{uu} , $K_{\phi\phi}$ and $K_{\psi\psi}$ are stiffness matrices due to mechanical, electrical and magnetic fields, respectively. The different elemental stiffness matrices of Eq. (10) for magneto-electro-elastic beam further defined as

$$\begin{aligned}
[K_{uu}^e] &= \int_v [B_u]^T [c] [B_u] dv; & [K_{u\phi}^e] &= \int_v [B_u]^T [e] [B_\phi] dv; & [K_{u\psi}^e] &= \int_v [B_u]^T [q] [B_\psi] dv \\
[K_{\phi\phi}^e] &= \int_v [B_\phi]^T [\varepsilon] [B_\phi] dv; & [K_{\phi\psi}^e] &= \int_v [B_\phi]^T [m] [B_\psi] dv; & [K_{\psi\psi}^e] &= \int_v [B_\psi]^T [\mu] [B_\psi] dv \\
K_{\phi u} &= K_{u\phi}^T; & K_{\psi u} &= K_{u\psi}^T; & K_{\psi\phi} &= K_{\phi\psi}^T
\end{aligned}$$

3. Results and discussion

A numerical calculation of a 3D magneto-electro-elastic beam is carried out with both piezoelectric and piezomagnetic phases which are considered as transversely isotropic. The axis of symmetry is oriented in z -direction. The material properties of different volume fraction of the piezoelectric phase are given in Table 1. The dimensions of the 3D magneto-electro-elastic beam used for analysis are $1.0 \times 0.1 \times 0.1$ m. The beam is subjected to uniform temperature rise of 100 °K with clamped-free boundary condition. To study the influence of product properties, the results are compared with pyroelectric and pyromagnetic properties, and conventional approach (MEE beam without considering pyroelectric and pyromagnetic properties).

3.1 Validation of the proposed formulation

A code has been developed to study the influence of pyroelectric and pyromagnetic properties on displacements, electric potential, magnetic potential, stresses, electric displacements and magnetic flux densities of 3D magneto-electro-elastic beam subjected to clamped-free boundary condition. For validation, the commercial finite element package ANSYS 13 is used. ANSYS cannot model piezomagnetic materials. The code has been validated for piezoelectric material model, without considering piezomagnetic coupling. The displacement components and electric potential due to uniform temperature rise for the proposed formulation are compared using ANSYS. From Fig. 2 it can be seen that, there is good agreement between the results obtained from the proposed formulation and ANSYS.

3.2 Influence of pyroelectric and pyromagnetic properties

Numerical studies are carried out with product properties and also the conventional approach (MEE beam without considering pyroelectric and pyromagnetic properties) on a MEE beam with uniform temperature rise of 100 °K applied under clamped-free boundary conditions. Two cases are studied here:

- Case I: Influence at volume fraction, $v_f = 0.5$ (50% of $BaTiO_3$) and
- Case II: Influence at different volume fractions, $v_f = 0.0, 0.2, 0.4, 0.6, 0.8, 1.0$

The influence of these product properties on displacements, electric potential, magnetic potential, stresses, electric displacements, and magnetic flux densities are studied.

3.2.1 Case I: Influence at volume fraction, $v_f = 0.5$

In the present study, the influence of product properties (pyroelectric and pyromagnetic) at volume

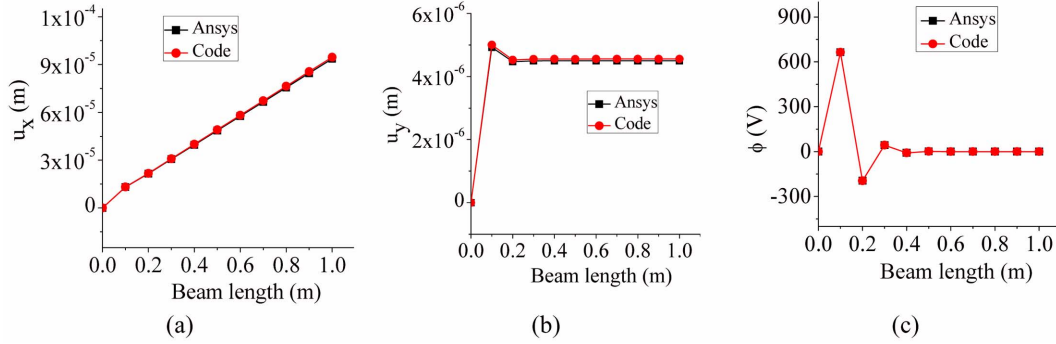


Fig. 2 Validation of (a) axial (u_x), (b) transverse y -direction (u_y) displacement components and (c) electrical potential (ϕ)

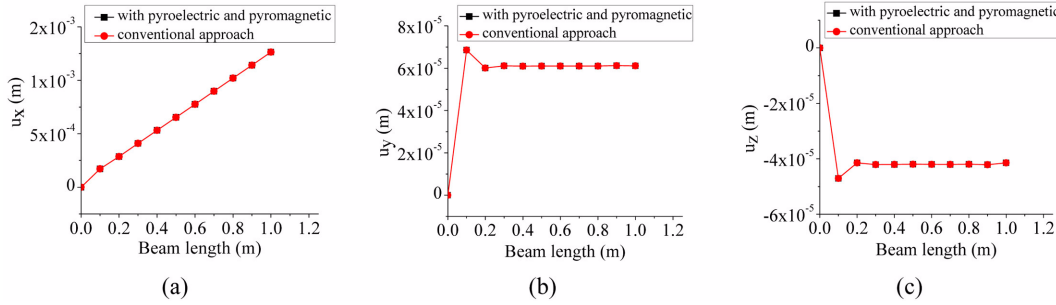


Fig. 3 Variation of (a) Axial (u_x), (b) transverse y -direction (u_y) and (c) transverse z -direction (u_z) displacement components

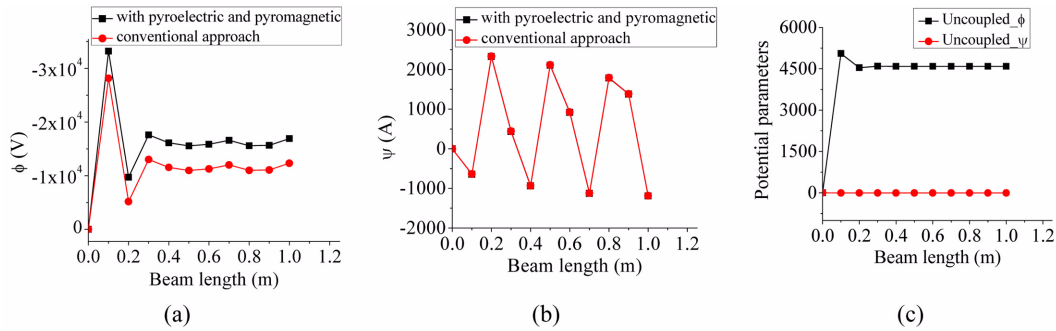


Fig. 4 Variation of (a) electric potential (ϕ), (b) magnetic potential (ψ) and (c) uncoupled electric (ϕ) and magnetic (ψ) potentials

fraction of $BaTiO_3$, $\nu_f=0.5$ on clamped-free boundary condition is carried out as Case I. The variation of axial (u_x), transverse y -direction (u_y), transverse z -direction (u_z) displacements are shown in Fig. 3, electric potential (ϕ) and magnetic potential (ψ) in Fig. 4, normal and shear stresses in Fig. 5, electric displacements in Fig. 6, and magnetic flux densities in Fig. 7 with ‘pyroelectric and pyromagnetic’ and conventional approach. It is observed that, there is no ‘pyroelectric and

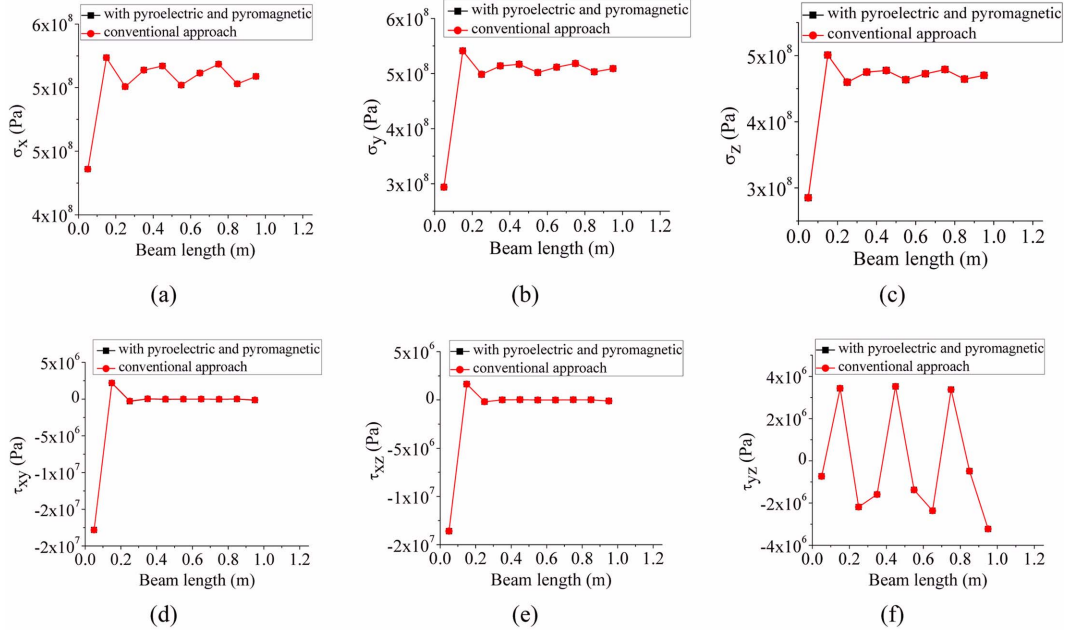
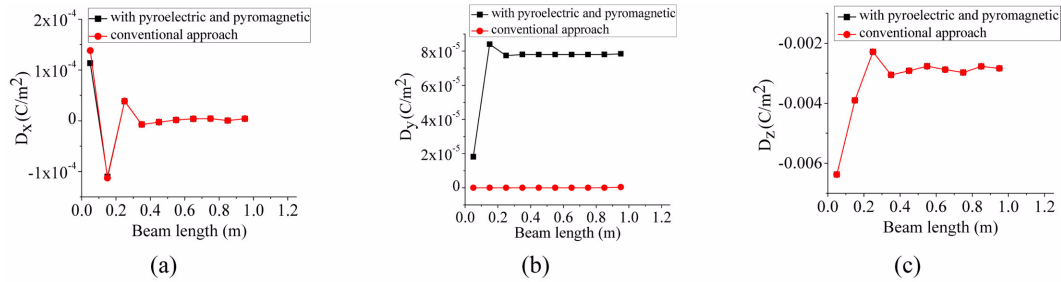


Fig. 5 Variation of (a)-(c) normal stress, and (d)-(f) shear stress components


 Fig. 6 Variation of (a) axial (D_x), (b) transverse y -direction (D_y) and (c) transverse z -direction (D_z) electric displacement components

pyromagnetic' effect on displacements, normal and shear stresses as shown in Figs. 3(a)-(c), and Figs. 5(a)-(f) respectively in comparison with the conventional approach. This is because the displacements in the system are governed by thermal loading directly which is given in Eq. (11) and the influence of electric and magnetic potentials indirectly.

In contrast, there is a significant increase in electric potential shown in Fig. 4(a), because it is directly governed by pyroelectric (Eq. (12)) and pyromagnetic (Eq. (13)) loadings and indirectly by thermal loading. Whereas there is no effect on magnetic potential even though τ (pyromagnetic coefficient) is greater than p (pyroelectric coefficient) by three orders of magnitude. This may be due to no effect of uncoupled magnetic potential (ψ) in comparison with uncoupled electric potential (ϕ) as shown in Fig. 4(c).

It is also seen that, there is a proportionate increase in electric displacement as shown in Fig. 6(b) and a small increase in magnetic flux density shown in Fig. 7(b), in the transverse y -direction

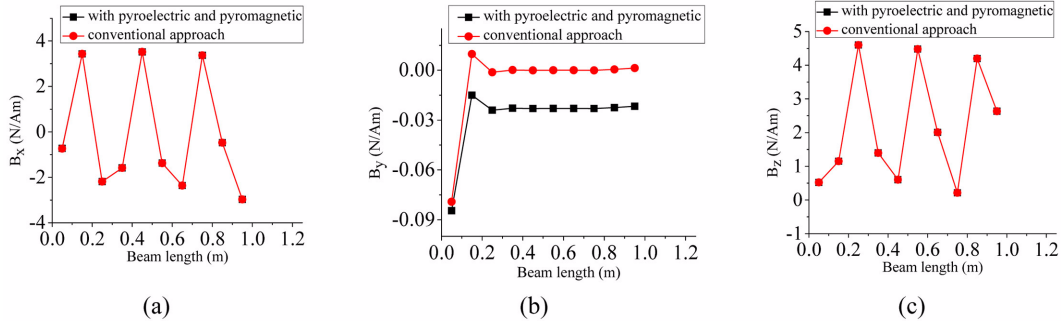


Fig. 7 Variation of (a) axial (B_x), (b) transverse y-direction (B_y) and (c) transverse z-direction (B_z) magnetic flux density components

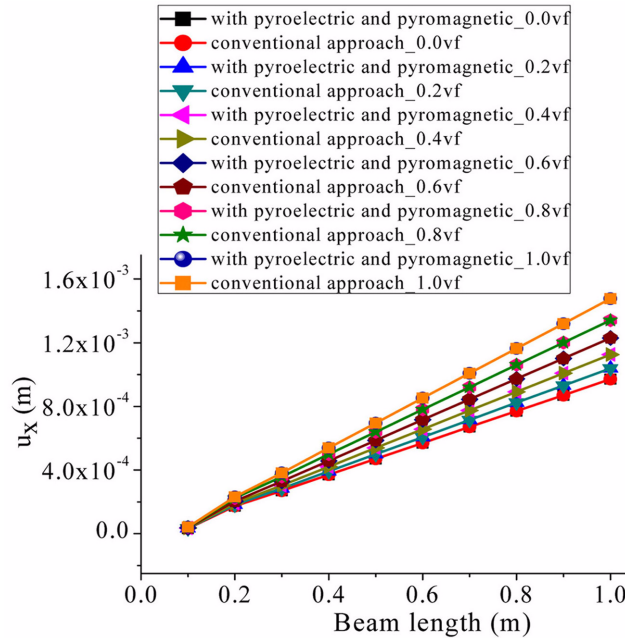


Fig. 8 Variation of axial displacement component (u_x)

respectively. This may be due to the contribution of increase in electric potential with ‘pyroelectric and pyromagnetic’ effect. No effect is observed in other components (axial and transverse z-direction) of electric displacement and magnetic flux density as shown in Figs. 6(a) and (c), and Fig. 7(a) and (c) respectively.

3.2.2 Case II: Influence at different volume fractions

In order to see the maximum influence of product properties on multiphase magneto-electro-elastic beam, the study is carried out at different volume fractions as Case II. The variation of axial (u_x) displacement and electric potential (\mathcal{D}) are shown in Figs. 8 and 9 respectively. It is seen that, the maximum value of electric potential observed at volume fraction $v_f=0.2$ due to ‘pyroelectric

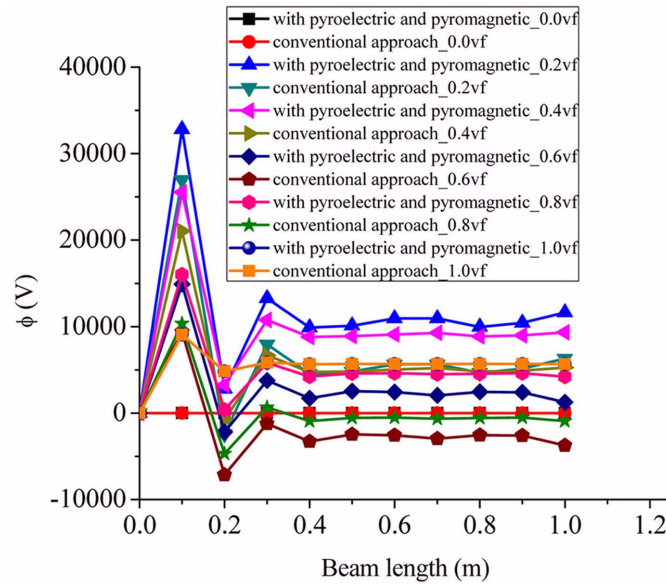


Fig. 9 Variation of Electric potential (ϕ)

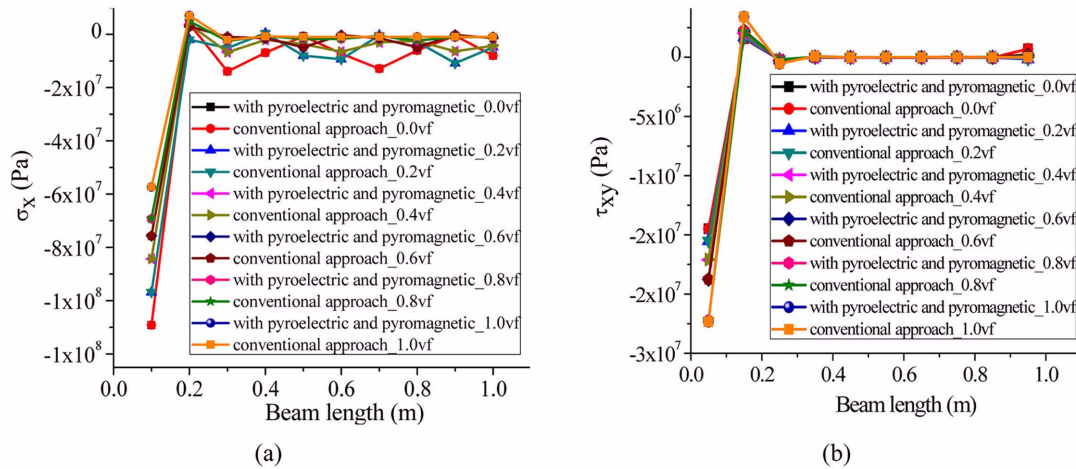


Fig. 10 Variation of (a) normal stress and (b) shear stress components

and pyromagnetic' effect. In contrast, no effect on displacements is observed with different volume fractions.

Comparison of stresses are shown in Fig. 10 and transverse y-direction electric displacement and magnetic flux density components are in Fig. 11. It is seen that, there is a proportionate increase in electric displacement observed at volume fraction $v_f=0.8$ (shown in Fig. 11(a)) and magnetic flux density at volume fraction $v_f=0.2$ (shown in Fig. 11(b)). It is also observed that, there is no influence of product properties on normal and shear stresses.

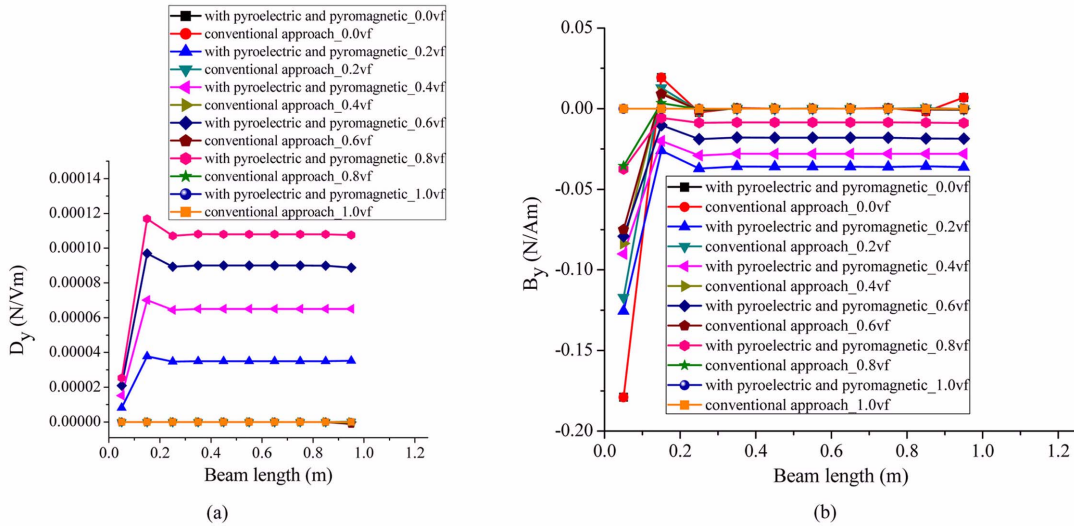


Fig. 11 Variation of transverse y-direction (a) electric displacement and (b) magnetic flux density components

4. Conclusions

The influence of pyroelectric and pyromagnetic properties on magneto-electro-elastic beam with different volume fractions under uniform temperature rise subjected to clamped-free boundary condition is studied as two cases. The Case I at volume fraction $v_f = 0.5$ (50% of $BaTiO_3$) and Case II at different volume fraction are analyzed to see the influence and maximum influence of product properties respectively. It was observed that,

- In present study the displacements and stresses are not much affected by ‘pyroelectric and pyromagnetic’ effect. This is because the displacements in the system are governed by thermal loading directly, and the influence of electric and magnetic potentials indirectly. Hence the indirect effects are negligible.

- In contrast, a significant increase in electric potential is observed. This is because the electric and magnetic potentials are directly governed by pyroelectric and pyromagnetic loadings, and indirectly by displacements. Hence pyroelectric and pyromagnetic effects have a direct effect, and thus influence the system significantly more.

- The overall comparison of different volume fraction (v_f) of $BaTiO_3$, the pyroelectric effect is maximum at $v_f = 0.2$.

References

- Aboudi, J. (2001), “Micromechanical analysis of fully coupled electro-magneto-thermo-elastic multiphase composites”, *Smart Mater. Struct.*, **10**(5), 867-877.
- Alibeigloo, A. (2010), “Thermoelasticity analysis of functionally graded beam with integrated surface piezoelectric layers”, *Compos. Struct.*, **92**(6), 1535-1543.
- Biju, B, Ganesan, N. and Shankar, K. (2011), “Dynamic response of multiphase magneto-electro-elastic sensors using 3D magnetic vector potential approach”, *IEEE Sen. J.*, **11**(9), 2169-2176.
- Bravo-Castillero, J., Rodriguez-Ramos, R., Mechkour, H., Otero, J. and Sabina, F.J. (2008), “Homogenization of

- magneto-electro-elastic multilaminated materials”, *Q. J. Mech. Appl. Math.*, **61**(3), 311-322.
- Buchanan, G.R. (2004), “Layered versus multiphase magneto-electro-elastic composites”, *Compos. Part B - Eng.*, **35**(5), 413-420.
- Challagulla, K.S. and Georgiades, A.V. (2011), “Micromechanical analysis of magneto-electro-thermo-elastic composite materials with applications to multilayered structures”, *Int. J. Eng. Sci.*, **49**(1), 85-104.
- Gornandt, A. and Gabbert, U. (2002), “Finite element analysis of thermopiezoelectric smart structures”, *Acta Mech.*, **154**(1-4), 129-140.
- Haozhong, G., Chattopadhyay, A., Li, J. and Zhou, X. (2000), “A higher order temperature theory for coupled thermo-piezoelectric-mechanical modeling of smart composites”, *Int. J. Solids Struct.*, **37**(44), 6479-6497.
- Huang, D.J., Ding, H.J. and Chen, W.Q. (2010), “Static analysis of anisotropic functionally graded magneto-electro-elastic beams subjected to arbitrary loading”, *Eur. J. Mech. A - Solid.*, **29**(3), 356-369.
- Kim, J.Y. (2011), “Micromechanical analysis of effective properties of magneto-electro-thermo-elastic multilayer composites”, *Int. J. Eng. Sci.*, **49**(9), 1001-1018.
- Kumaravel, A., Ganesan, N. and Sethuraman, R. (2007), “Steady-state analysis of a three-layered electromagneto-elastic strip in a thermal environment”, *Smart Mater. Struct.*, **16**, 282-295.
- Ootao, Y. and Ishihara, M. (2011), “Exact solution of transient thermal stress problem of the multilayered magneto-electro-thermoelastic hollow cylinder”, *J. Solid Mech. Mater. Eng.*, **5**(2), 90-103.
- Ootao, Y. and Tanigawa, Y. (2005), “Transient analysis of multilayered and magneto-electro thermoelastic strip due to nonuniform heat supply”, *Compos. Struct.*, **68**(4), 471-9.
- Pan, E. (2001), “Exact solution for simply supported and multilayered magneto-electro-elastic plates”, *J. Appl. Mech. - T ASME*, **68**, 608-618.
- Pan, E. and Wang, R. (2009), “Effects of geometric size and mechanical boundary conditions on magnetolectric coupling in multiferroic composites”, *J. Phys. D. Appl. Phys.*, **42**, 245503.
- Sunar, M., Al-Garni, A.Z., Ali, M.H. and Kahraman, R. (2002), “Finite element modeling of thermo-piezomagnetic smart structures”, *AIAA J.*, **40**, 1846-51.